Transition Radiation Detector for the GlueX experiment

Alexander Austregesilo, Eugene Chudakov, Sergey Furletov, and Lubomir Pentchev
Thomas Jefferson National Accelerator Facility,
Newport News, Virginia 23606, USA

Sean Dobbs
Florida State University, Tallahassee, Florida 32306, USA

(Dated: January 29, 2022)

Abstract

We propose to build a Transition Radiation Detector (TRD) with Gaseous Electron Multiplier (GEM) amplification, referred as GEM-TRD, to improve the electron-pion separation in the GlueX experiment. It will allow to study precisely reactions with electron-positron pairs in the final states; such reactions like J/ψ photoproduction near threshold have significant impact in many fields of the particle physics. The document discusses the motivation for such an upgrade and the physics goals, together with the technical description of the proposed detector and the electronics. Requirements for the GEM-TRD gas system are specified. Finally, estimates of the costs and the proposed time line are presented.

CONTENTS

I. EXECUTIVE SUMMARY

Important features of the GlueX detector include full acceptance, charge and neutral particle registration, precise knowledge of the photon beam energy, and high-rate electronics and DAQ, however it has limited particle-identification capabilities. A DIRC detector was built for the phase-II of the GlueX experiment and used for pion/kaon separation that will extend the GlueX program by including strangeness physics. Another important extension of the program would be the di-electron physics. The GlueX detector has the unique possibility to study the J/ψ photoproduction off the proton near threshold in the full kinematic space. As the J/ψ-proton interaction is mediated predominantly by gluons, such studies allow to probe the gluonic content of the proton: mass radius, anomalous contribution to the mass of the proton, the gluonic GPD; all these properties are not accessible with electro-magnetic probes. First results of the J/ψ photoproduction near threshold [1], published by GlueX in 2019, collected already 100+ citations. Such studies, however, are limited by the huge pion background that can mimic the electron-positron pairs used to identify the J/ψ particle.

The electro-magnetic calorimeters are not enough to suppress the pion background. The addition of the proposed Transition Radiation Detector (TRD) employing Gaseous Electron Multiplier (GEM) technology, or GEM-TRD, has the following advantages:

- As an independent low-mass detector, it can be placed in front of the electro-magnetic calorimeter allowing to measure precisely the calorimeter's pion suppression efficiency, which is critical for the above studies. At the same time the calorimeter can be used to study the efficiency of the GEM-TRD.

- The proposed detector will give a factor of 10 pion suppression allowing to study the Bethe-Heitler electro-magnetic process that is fully calculable and has the same e^+e^-p particles in the final state as the J/ψ photoproduction. This will reduce the systematic uncertainties of the latter reaction significantly, e.g. for the total normalization from 27% to less than 10%.

- The detector will minimize the pion contamination in the J/ψ events to a level at which amplitude analysis can be performed reliably. The null results [1, 2] of the search in the J/ψ photoproduction for the LHCb pentaquarks [3, 4] mean that, if they exists, we have limited sensitivity. Therefore, amplitude analysis in the whole kinematic space might be crucial for identifying such states or setting much lower limits on their existence.

- The detector will allow also measurements of other interesting reactions with di-electrons in the final state, like TCS, ... (Sean ...)
- The GEM-TRD works also as a Time Projection Chamber (TPC) giving a track segment within the drift volume of the detector. This will improve the pattern recognition and the momentum resolution which is limited in the forward direction and, at the same time, help the performance of the DIRC detector by providing it with a precise tracking just in its front.

Most of the results in support of the physics program with this detector are based on measurements and data-driven simulations. The specifications and the proposed design of the detector are results of many years of tests with prototypes.

The building of the GEM-TRD includes several stages: (1) measurements with small prototypes to prove the principle and make initial detector design (already finished), (2) manufacture and test a large-scale prototype (2021-2023 in progress), (3) design and produce a gas recirculating system (2022-2023), (4) manufacture one of the two chambers of the final detector and use it during the phase-II of the GlueX experiment (2023-2025), (5) manufacture the second chamber (2025-2026).

We estimate the total price of the full detector to be in the range of \$565−810k, depending on the electronics. For the best performance of the detector we propose to have 4.9k readout channels. If equipped with the flash ADCs that are used currently in the drift chambers of the GlueX experiment, we estimate a price of \$100 per channel, or \$490k for the whole electronics. Another option is to use a modern version of our electronics, that is now under development that may cut the price by a half. We estimate the price of the gas system and the detector itself to be \$150k and \$120k respectively. Additional expenses of \$50k include the mechanical infrastructure.

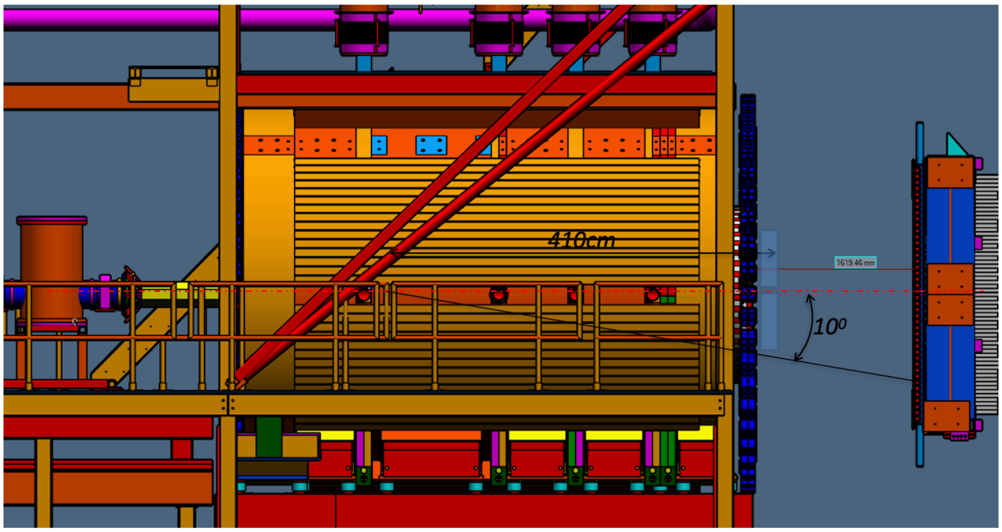

FIG. 1: Side view showing the approximate position of the proposed GEM-TRD detector (light blue boxes), at 410 cm downstream of the target, covering 86% of the forward GlueX acceptance of $\sim 10°$ polar angle. The DIRC detector not in the plot.

II. THE GEM-TRD DETECTOR

The proposed detector will be placed in the forward region of the GlueX detector just at the downstream face of the solenoid, in front of the DIRC and FCAL, see Figs. 1,2. It will consists of two separate chambers, each providing 1392×528 mm^2 sensitive area. The frames of the chambers holding the front-end electronics will be outside of the acceptance (Fig. 2).

The detector has a radiator layer 15 cm thick, followed by a 2 cm drift volume, and a GEM stage combined with a readout board. The principle of operation is illustrated in Fig.3a. The Transition Radiation (TR) photons in the keV region produced by the electrons in the radiator are absorbed by the Xe gas mixture in the drift volume emitting electrons that drift to and are amplified by the GEM. The signals are readout from X- and Y-strips on the readout board. The horizontal strips are separated in the middle and readout from the left and right side of the chambers (Fig. 2). The strip pitch is 1 mm, resulting in $2,448$ electronic channels per chamber, or $4,896$ in total. The signals are amplified on-board and

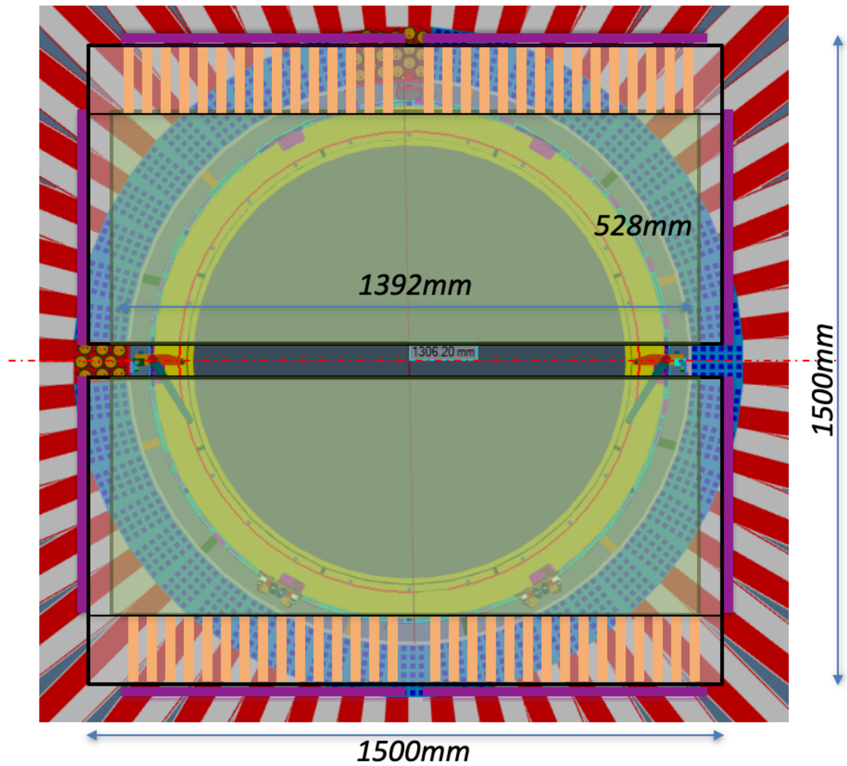

FIG. 2: Front view of the GEM-TRD detector placed at the face of the solenoid magnet. It consists of two separate chambers with 1392×528 mm^2 sensitive area. All the frames holding the front-end electronics (purple thick lines) of sizes $\sim 1500 \times 1500$ mm^2 are outside of the GlueX forward acceptance.

then digitized with flash ADCs. We assume using the same electronics as for the GlueX drift chambers: GASII [5] preamps and flashADC-125 [6], however alternative better and cheaper options will be discussed bellow. Thus we record the energy deposition along the track (measured by the drift time) that has different profile for the TR photons absorbed predominately at the entrance, and the track ionization that has uniform distribution, see Fig.3b. At the same time such detector works as a Time Projection Chamber, allowing to reconstruct the track segment within the drift volume.

The main parameters of the GEM-TRD detector are given in Table I. They are based on tests with small prototypes (10×10 cm^2) done during the past several years, as discussed in the next section, and are preliminary. Further optimization of the detector will be done with a large-scale prototype that will be built and tested during the 2022 and 2023 running periods.

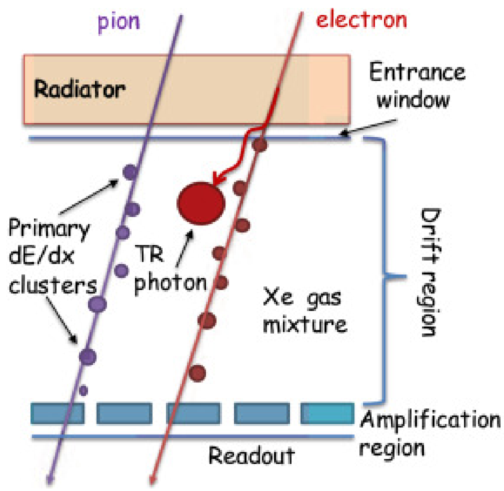

(a) GEM-TRD principle

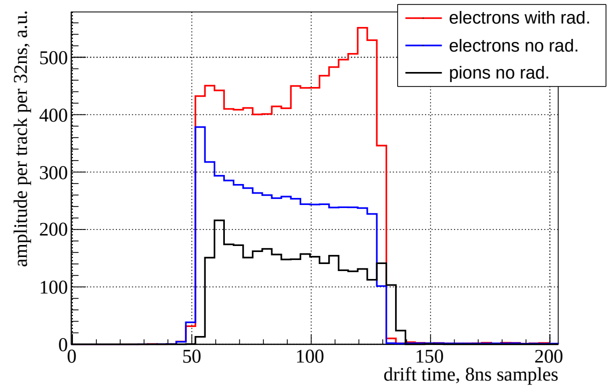

(b) Amplitude profiles for electrons with and without radiator and pions; data from studies with small prototypes

FIG. 3

parameter	value	comment
sensitive area	$2 \times (1392 \times 528\ \mathrm{mm}^2)$	two separate chambers
frame-free area	$1500 \times 1500\ \mathrm{mm}^2$	except some minimal support
distance from the target	4100 mm	
forward acceptance coverage	86%	for e^+e^- invariant mass > 1.2 GeV
radiator thickness	150 mm	
drift volume thickness	20 mm	
total detector thickness	$< 4\%$ R.L.	
drift field	1.5 kV/cm	
gas mixture	Xe/CO_2 90/10	
maximum drift time	800 ns	
gas amplification	$\sim 5.10^4$	
strip types	X and Y	on the same layer with capacitive coupling
strip pitch	1 mm	
readout channels	4,896	2,448 per chamber
GASII pre-amps (24 channels)	204	102 per chamber
GASII amplification	2.4 mV/fC	
flashADC-125 (72 channels)	68	34 per chamber
VXS crates	5	

TABLE I: Main parameters of the GEM-TRD detector.

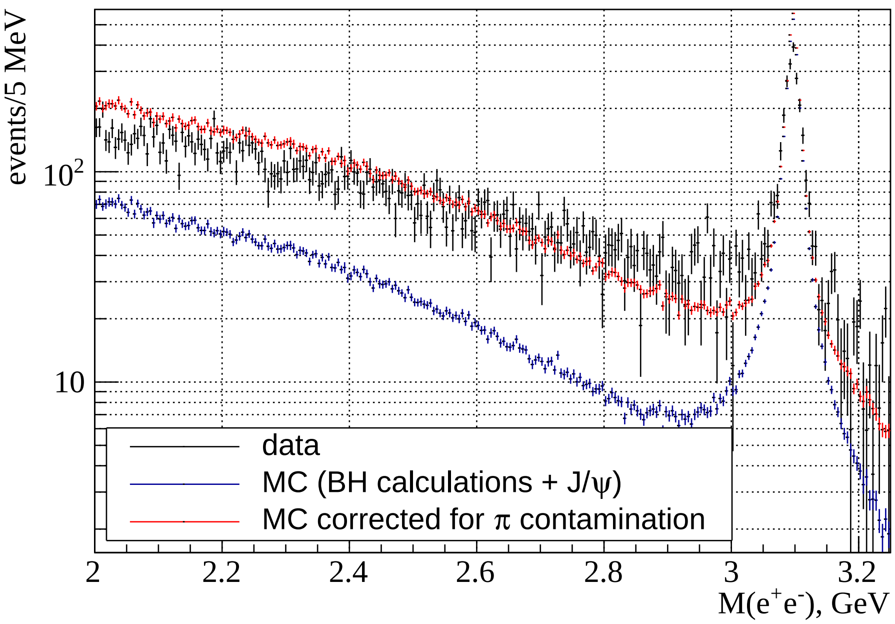

FIG. 4: The e^+e^- invariant mass spectrum from data compared to Monte Carlo simulations that use absolute BH calculations (as well as the J/ψ photoproduction normalized to the data) and their modification that adds the pion background (see text).

III. PHYSICS OBJECTIVES

The best approach to extract the absolute J/ψ cross-sections is to use the BH process for normalization using the formula [1]:

$$\sigma = \frac{N_{J/\psi}}{N_{BH}} \frac{\sigma_{BH}}{BR_{J/\psi}} \frac{\varepsilon_{BH}}{\varepsilon_{J/\psi}} , \tag{1}$$

where only the relative efficiency, $\varepsilon_{BH}/\varepsilon_{J/\psi}$, of the J/ψ and BH processes enters; here N_{BH} and $N_{J/\psi}$ are the yields of the corresponding processes, σ_{BH} – the calculated BH cross-section, and $BR_{J/\psi}$ – the branching ratio of the $J/\psi \to e^+e^-$ decay.

Fig.4 illustrates the problem with the pion background in the GlueX detector. It shows the e^+e^- invariant mass spectrum from the data (black), compared to simulations that include absolute calculations of the BH process [7–9] in the continuum and the J/ψ peak normalized to the data (blue). For this plot we apply all the selections as explained in [1]. Most importantly, 3σ cuts are applied around the peaks in the p/E distributions (p is the momentum and E the energy deposited in the corresponding calorimeter, BCAL and FCAL) for both, the electron and the positron candidates. Additional selection is applied on the signal from the first layer of BCAL, that works as a pre-shower. As we register all the final state particles and have very good precision for the beam photon energy, we can apply a Kinematic Fit (KF) that constrains the four momenta and the vertex position of the final state particles. The KF reduces significantly the background, as discussed below.

Thus, after all selections applied, the pion background is of the same order as the signal and, therefore, we have to use some statistical procedures to estimate the background and extract the BH yields. The result of such procedure is shown on the same plot – the red points in Fig.4 correspond to the simulations (blue) to which the pion background is added using the signal-to-background ratios in Figs.5a,5b. Examples of p/E fits used to estimate these ratios from the data are given in the Appendix.

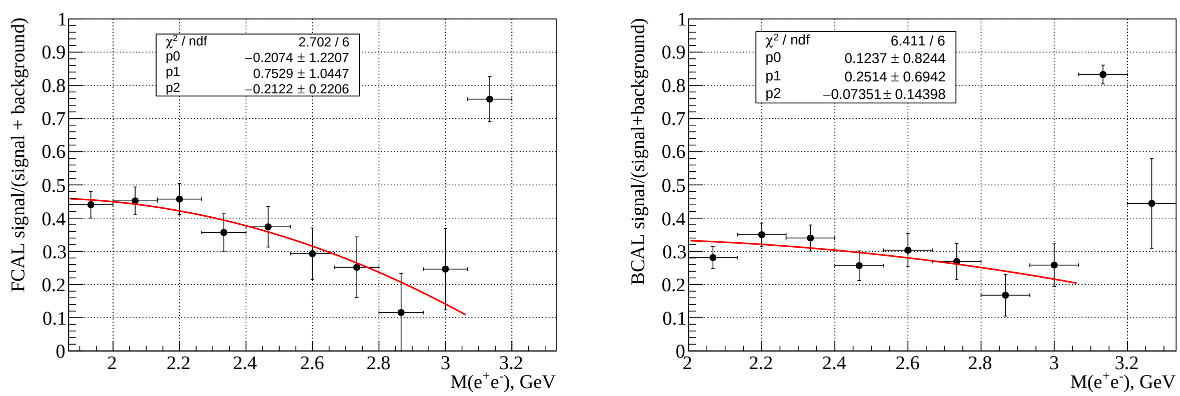

(a) FCAL (b) BCAL

FIG. 5: The signal to (signal+background) ratio for the two calorimeters as function of the e^+e^- invariant mass fitted with a polynomial.

In Fig.6 we plot the e^+e^- mass spectra for two cases, when at least one lepton goes forward and when both leptons are registered in the BCAL. The pion background is much more significant in the forward direction, where the GEM-TRD will be installed. This can be explained by the fact that background reactions like $\gamma p \to \Delta\pi \to p\pi\pi$ (Δ can be any other nuclonic resonance) will produce predominately one forward pion and one backward coming from the target excitation.

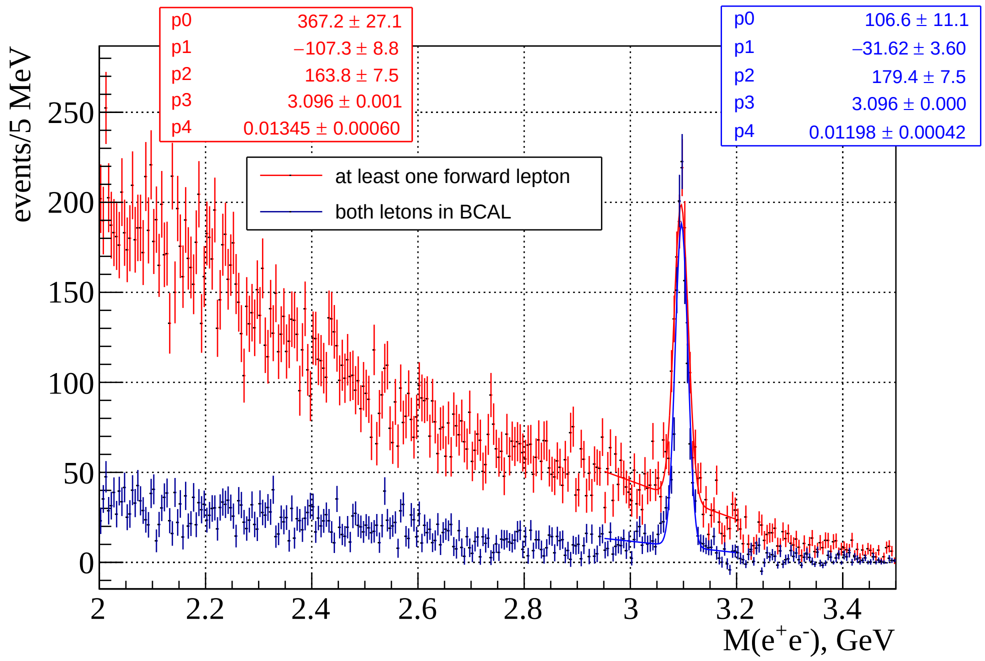

FIG. 6: The e^+e^- invariant mass spectrum from data in case of at least lepton goes in the forward direction, and when both leptons are registered in BCAL. The background below the J/ψ peak $\pm 3\sigma$ in forward direction is 65%.

A. Improving the systematics of the J/ψ photoproduction using GEM-TRD

1. *Pion rejection efficiency*

The simulation of the calorimeter response to pions is not perfect. Thus, the selections applied to data and simulations may have different efficiencies. This is seen when comparing the p/E distributions from data and MC (see Appendix). At the same time, the p/E cuts are the most important in rejecting the pions. The fitting procedures to extract the e^+e^- yields are very sensitive to these selections and suffer from instability, especially for FCAL due to the steep background. One can try to do effective corrections to the simulations based on the data, however, due to the momentum and angular dependence of these correction, this is not possible in practice. Therefore, so far, we were not able to attribute any systematic error related to the pion rejection efficiency. The best solution would be to use the GEM-TRD in front of the FCAL to create a clean sample of electrons and measure the FCAL rejection efficiency. For that we don't need the whole acceptance of the GlueX detector and propose to do such measurements, first, with one chamber only – see the timeline of the proposal in Sec.VII. Then, the results of these measurements can be used for the whole data set to

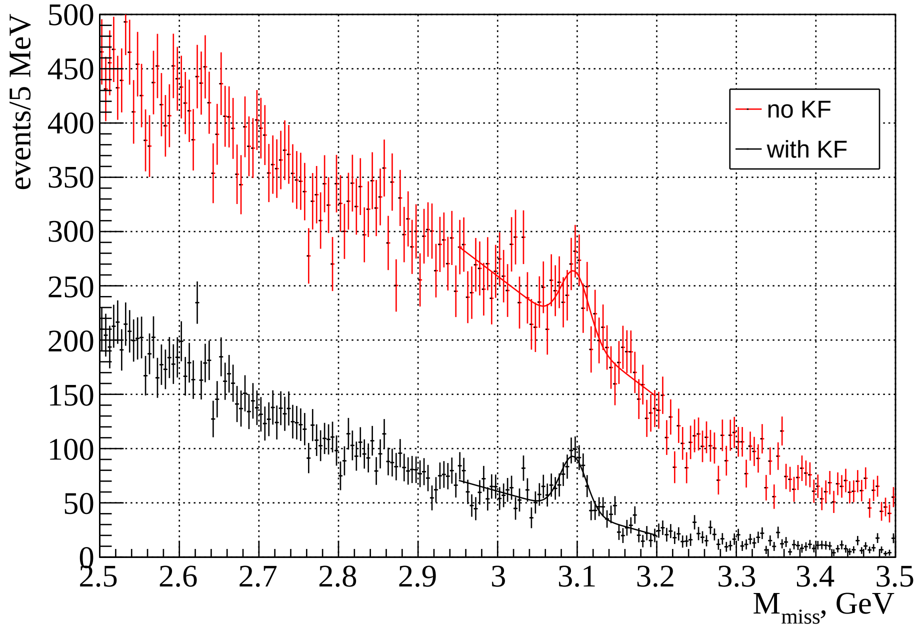

FIG. 7: The missing mass off the recoil proton from the data with and without Kinematic Fit (KF), with at least one forward lepton.

improve the simulations and assign a realistic systematic error.

2. The efficiency of the Kinematic Fit

The Kinematic Fit (KF) cuts more than 50% of the final state particle candidates, therefore potentially it is a significant source of systematic errors. However, it is needed because it improves the e^+e^- mass resolution and reduces the background significantly, especially in the forward direction. As for the mass resolution, there is an alternative of using the measured electron/positron momenta and angles. Fig.7 shows the e^+e^- mass spectrum as measured by the missing mass off the recoil proton with and without the KF, in the case of at least one lepton in the forward direction. The mass resolution is as good as the standard reconstruction, however the background without the KF is significant and doesn't allow to extract the cross sections reliably, as the fluctuation of the background are similar in size to the J/ψ peak. Again, the use of the GEM-TRD would reduce the background to about 10% allowing to do studies with and without the KF and measure its efficiency.

3. BH normalization

Fig.8 compares the measured BH cross sections to the absolute calculations, as function of the invariant mass. One can see from Fig.8b that the data/MC ratio is not constant and

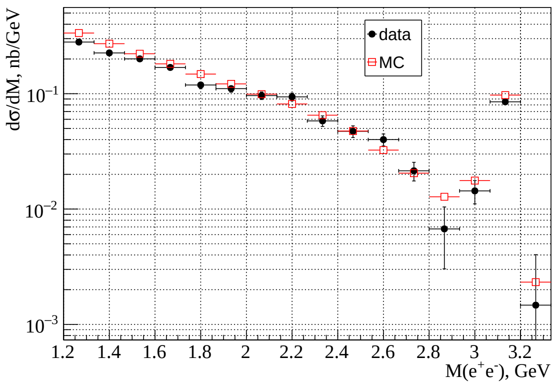

(a) BH cross-sections from data and MC.

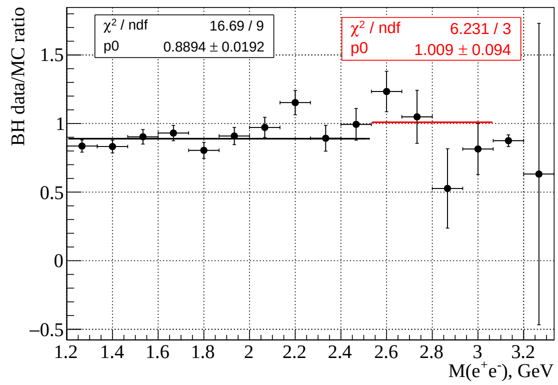

(b) BH data/MC ratio from Fig.8a fitted with constants in two regions.

FIG. 8: BH cross-section vs invariant mass: data vs MC.

shows a tendency of increasing towards the J/ψ peak, however with a significant uncertainty. Based on such studies we estimated [1] a contribution to the normalization uncertainty of about 25%, which is the dominant contribution to the systematics. We suspect that such data-MC inconsistency comes from the problems discussed in the previous subsections, the poor knowledge of the pion rejection and the KF efficiencies. In addition, we found that the errors of the cross section are dominated by the background fluctuations when fitting the p/E distributions (see Appendix). If we assume no pion background, the errors will be defined simply by the number of events, then our estimation of the normalization uncertainty would go down below 10%.

B. Amplitude Analysis of the J/ψ photoproduction and search for the LHCb pentaquarks

If the LHCb pentaquarks [3, 4] exist, they should be seen in the s-channel of the J/ψ photoproduction [10–12]. The negative results coming from JLab [1] mean that indeed, if such states exist, we need more precise tools to identify them. Performing amplitude analysis over the whole kinematic space has the potential to uncover such states, or set much lower

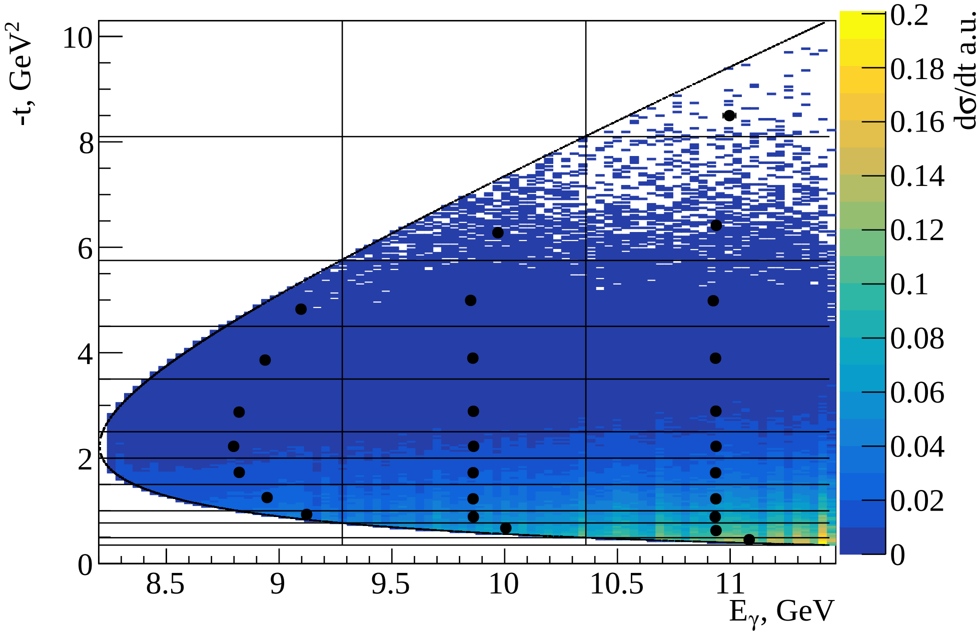

FIG. 9: The coverage of the kinematic space of the J/ψ photoproduction near threshold, with bins where GlueX will provide measurements of the $2D$ differential cross section. Shown are results from simulations, just for illustration.

limits on their existence. The GlueX detector has acceptance in the full kinematic range next to the threshold where the pentaquark region is, see Fig.9. However, the amplitude analysis requires knowledge of the amplitudes of the contributing reactions, including the background which is significant especially in forward direction, where it reaches 65% within 3σ of the J/ψ peak, see Fig.6. The GEM-TRD will reduce the pion contamination for the J/ψ events to about 5% that will make the amplitude analysis much more reliable.

(expect contribution from Alex ...)

C. Other di-electron reactions to be studied with GlueX

... TCS (including beam asymmetries?) ... expect contribution from Sean ...

D. Improving the tracking with the GEM-TRD

... Lubomir will work on this ..

IV. STUDIES WITH PROTOTYPES

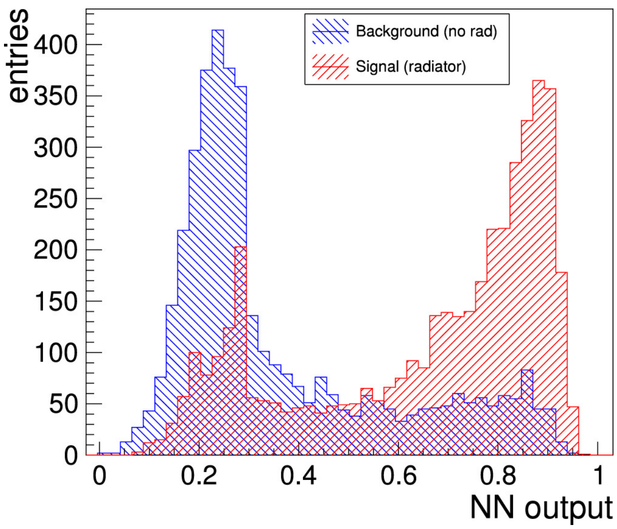

(a) Neural Network (NN) output for electrons with and without radiator

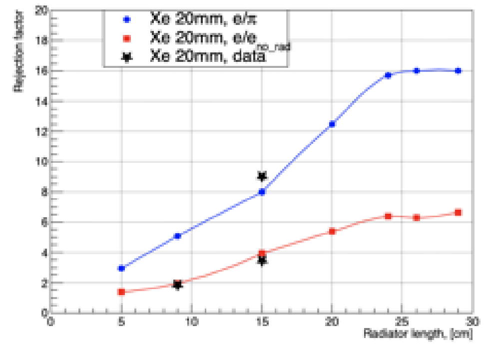

(b) Pion rejection factor from data (stars) and simulations from radiator/no radiator (red) and electron/pion (blue) comparison; data from studies with small prototypes

FIG. 10

Studies with small ($10 \times 10\text{cm}^2$) prototypes have been done during 2018-2021. They were performed both with electrons, at one of the Pair Spectrometer arms, and with pions in the forward GlueX acceptance, downstream of the magnet and in front of the DIRC detector. Some results of these measurements were presented already in Sec.II, showing the timing profile of the detector response for electrons with/without radiator and for pions, Fig.3b. Event-by-event analyses using neural network were done (Fig.10a, Fig.10b) demonstrating a factor of ~ 4 effect of the radiator with electrons, and ~ 10 pion rejection factor, the later based on experiments with electrons at pions done separately.

Such measurements proved the principle of using GEM technology for TR detectors. At the same time they helped to specify the parameters of next, large-scale prototype. This prototype will cover a quarter of the final detector (Fig.11), allowing to be used for real physics data taking. It will be produced under a contract with UVA that already started. We will use existing spare electronics to test it during 2022-2023.

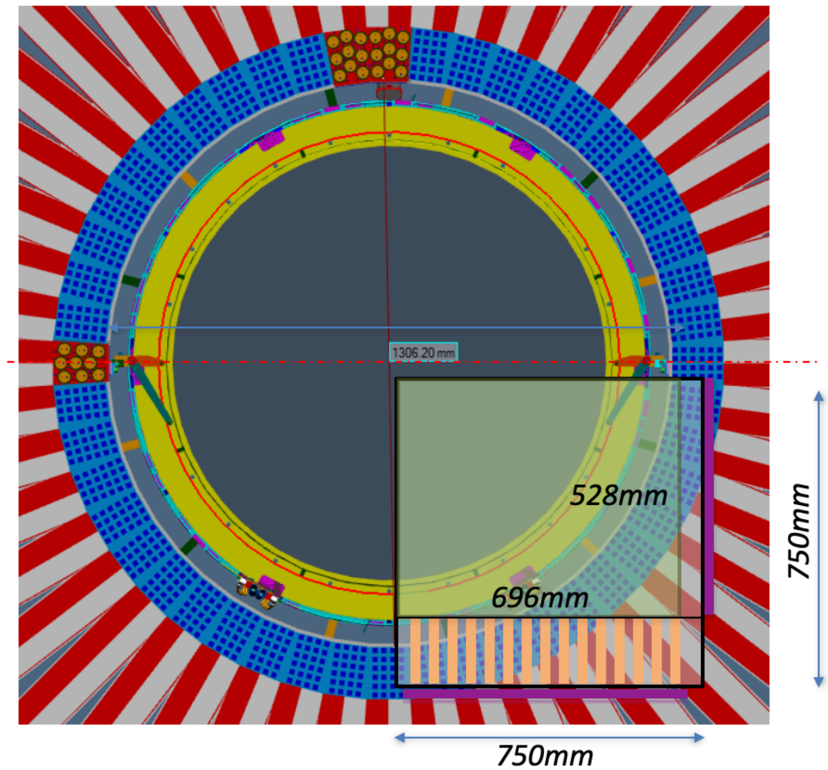

FIG. 11: Front view of the GEM-TRD large-scale prototype that has 696 × 528 mm^2 sensitive area.

V. GAS SYSTEM REQUIREMENTS

The high price of the Xe gas requires system that recirculates and purifies the gas mixture. The principle diagram of such system is shown in Fig.12. Each GEM-TRD module has two gas volumes - the main one filled with Xe/CO_2 gas mixture of 90/10% containing the drift and the amplification volumes, and the second one for the radiator filled with CO2. The thickness of the drift and amplification volume is 20 mm and 10 mm respectively. Thus, we estimate the Xe/CO_2 gas volume to be 25 l per chamber, or 50 l in total. For the CO_2 volume it has a thickness of 150 mm or 125 l per module and 250 l total. For the Xe/CO_2 volume we aim to have 8 volume exchanges per day, i.e. 20 l/h. The CO_2 volume can be exchanged once per day or 5 l/h.

The entrance and exit gas windows will be made of 100 μm Mylar, possibly enforced with Rochacell material. The detector will allow operation with overpressure between 0.5 and 2 mbar. The two gas volumes will be separated by 50 μm Mylar, covered with 1 μm Al. To limit the variations of the drift field, we require the pressure difference between the two gas

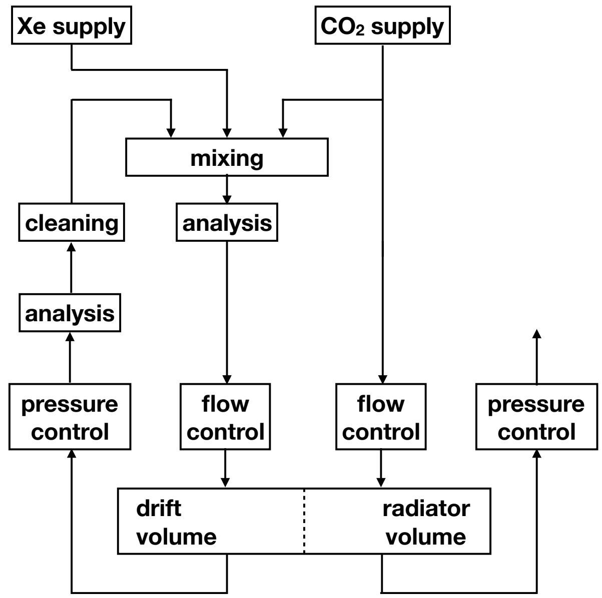

FIG. 12: Principle diagram of the gas recirculating system.

volumes to be less than 0.2 mbar.

Oxygen contamination and water vapor should be kept less than 50 ppm, to minimize the electron recombination in the drift volume. The Nitrogen contamination should be kept less than 0.5%.

The elements of the gas system that operate above 1 bar should be kept in a separate gas room, elevated approximately 7 m above the detector. They will be connected to the detector with gas lines of about 50 m length.

The parameters and requirements of the gas system are summarized in Table II.

item	requirement	comment
total Xe/CO_2 gas volume	50 l	
total CO_2 gas volume	250 l	
Xe/CO_2 gas flow	20 l/h	
CO_2 gas flow	5 l/h	
Operating overpressure	$0.5 - 2$ mbar	
Pressure difference b/n two volumes	< 0.2 mbar	
Oxygen contamination	< 50 ppm	
water vapor	< 50 ppm	
Nitrogen contamination	$< 0.5\%$	

TABLE II: General parameters and requirements for the GlueX TRD gas system.

VI. ELECTRONICS

We consider two options for the electronics. We can use the same electronics as for the GlueX drift chambers: GASII [5] preamps and flashADC-125 [6]. ......

The alternative is ... .

Comparison between the two ......

Cost estimates ......

(expect contribution from Sergey...)

VII. COST ESTIMATES AND TIMELINE

The estimated cost for the whole detector is summarized in Table.III. It is dominated by the electronics and the two options discussed in the previous section are considered. The price of the detector itself is based on the contract for producing the large scale prototype, and the experience of building large GEM chambers. The gas system price was discussed with experts from CERN.

item	price, $k	comment
electronics, option 1 (4,900 channels)	490	using existing pre-amp and fADC
electronics, option 2 (4,900 channels)	245	using modern design, under development
design and manufacture two TRD chambers	120	
gas recirculating system	150	
mechanical support and infrastructure	50	
total option 1	810	
total option 2	565	

TABLE III: Cost estimate for the whole GEM-TRD detector for two electronics options.

The general timeline of the proposed GEM-TRD project is shown in Table.IV. The prototyping with small detectors proved the principle of using GEM technology for TR detectors and helped to formulate the specifications for the next large-scale prototype. A contract with UVA was signed to design and produce the large-scale prototype, that we intend to test during the 2022-2023 running periods. At the same time we plan to develop and produce the gas system. Based on the result with the large prototype we will finalize the detector design. The first chamber is planned to be manufactured and used during the phase-II of the GlueX experiment in 2023-2025. Even covering half of the acceptance, it will allow to measure the calorimeter rejection efficiency and evaluate the KF, which results can be applied to the whole data set. In 2025-2026 we plan to produce second chamber and finish the project.

VIII. APPENDIX

Examples of the p/E fits in bins of energy are given in Fig.13 for BCAL and in Fig.14 for FCAL.

year	item	comment
2018-2021	tests with small prototypes	finished
2021-2023	produce and test large-scale prototype	in progress
2022-2023	design and produce gas system	
2023-2025	produce and evaluate one chamber	use during GlueX phase-II
2025-2026	produce and install the second chamber	

TABLE IV: General timeline of the GEM-TRD project.

[1] A. Ali et al. (GlueX collaboration), Phys. Rev. Lett. **123**, 072001 (2019).

[2] S. Joosten, Talk at 9th Workshop of the APS Topical Group on Hadronic Phtsics (2021).

[3] R. Aaij et al. (LHCb collaboration), Phys. Rev. Lett. **115**, 072001 (2015).

[4] R. Aaij et al. (LHCb collaboration), Phys. Rev. Lett. **117**, 082002 (2016).

[5] F. Babosa, https://halldweb.jlab.org/doc-private/DocDB/ShowDocument?docid=1364 The GAS-II/GPC-II GlueX Preamp Card Preliminary Test Results (2009).

[6] G. Visser, D. Abbot, F. Barbosa, C. Cuevas, H. Dong, E. Jastrzembski, B. Moffit, and B. Raydo, in *IEEE Nuclear Science Symposuim & Medical Imaging Conference* (IEEE, 2010) pp. 777–781.

[7] E. Berger, M. Diehl, and B. Pire, Eur.Phys.J.C **23**, 675 (2002).

[8] R. Paremuzyan, private communication (2017).

[9] R. Jones, private communication (2018).

[10] V. Kubarovsky and M. B. Voloshin, Phys. Rev. D **92**, 031502 (2015).

[11] M. Karliner and J. Rosner, Phys. Lett. B **752**, 329 (2016).

[12] A. Blin, C. Fernandez - Ramirez, A. Jackura, V. Mathieu, V. Mokeev, A. Pilloni, and A. Szczepaniak, Phys. Rev. D **94**, 034002 (2016).

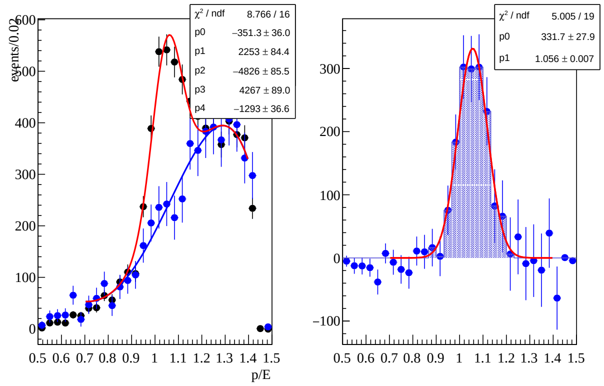

(a) BCAL bin 4 $8.74 < E_\gamma < 8.92$ GeV

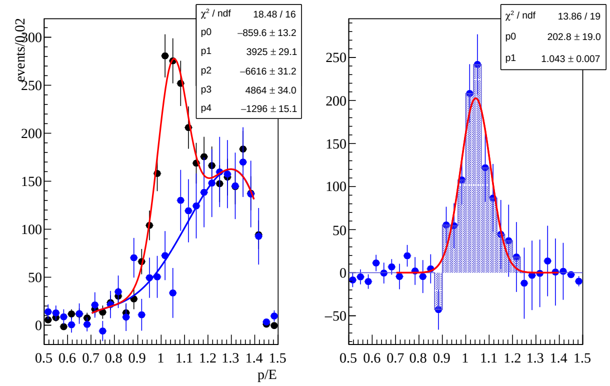

(b) BCAL bin 5 $8.92 < E_\gamma < 9.10$ GeV

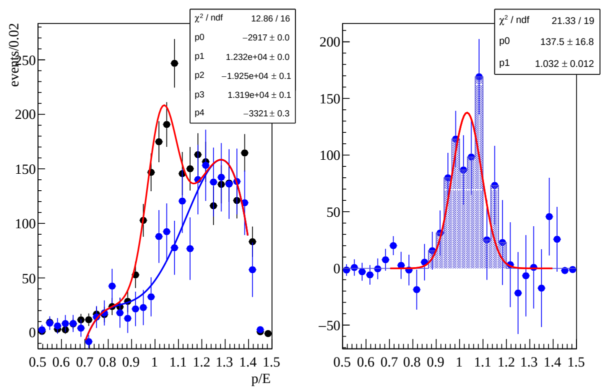

(c) BCAL bin 6 $9.10 < E_\gamma < 9.28$ GeV

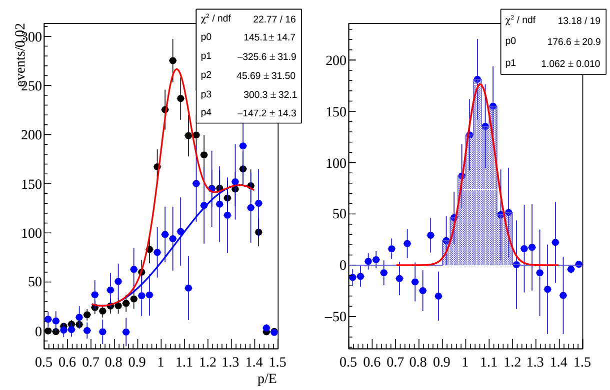

(d) BCAL bin 7 $9.28 < E_\gamma < 9.46$ GeV

FIG. 13: Fits of p/E distributions for BCAL for four energy bins. In the left panel of each plot the blue points fitted with the blue curve represent the background distribution, while the total distribution is shown with black points fitted with a Gaussian (fixed σ) plus the background polynomial (p0-p4 parameters); the three fitted parameters are the normalization coefficients of the Gaussian and the polynomial and the mean of the Gaussian. The right panel is the difference between the black and blue points from the left panel, fitted with a Gaussian with fixed width (p0, p1 - amplitude and mean); the sum of the shaded points ($\pm 3\sigma$) is used as an estimate of the signal.

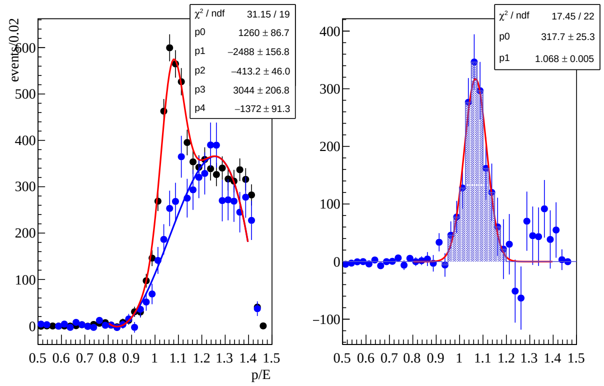

(a) FCAL bin 4 $8.74 < E_\gamma < 8.92$ GeV

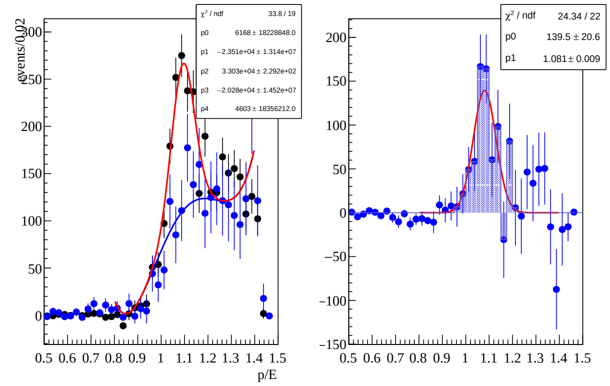

(b) FCAL bin 5 $8.92 < E_\gamma < 9.10$ GeV

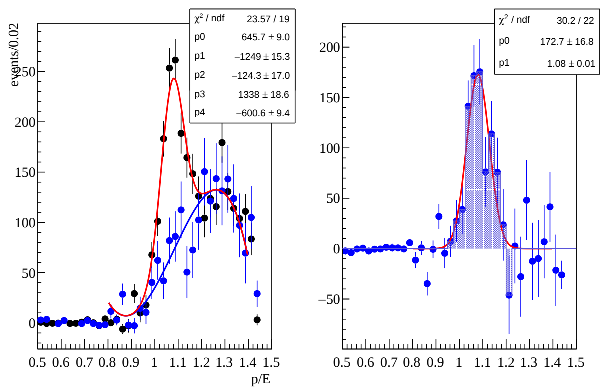

(c) FCAL bin 6 $9.10 < E_\gamma < 9.28$ GeV

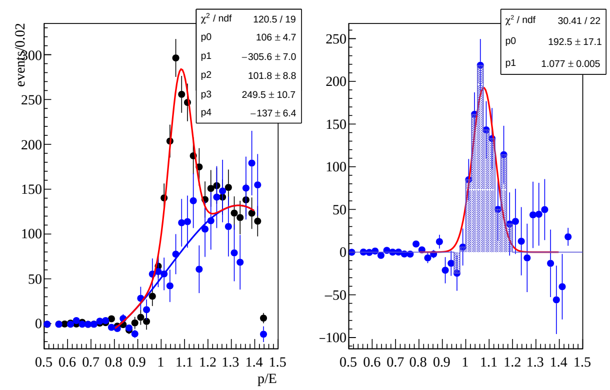

(d) FCAL bin 7 $9.28 < E_\gamma < 9.46$ GeV

FIG. 14: Same as in Fig.13 but for FCAL.